



UNIVERSITY OF
LIVERPOOL

USE OF SCANNING TUNNELLING MICROSCOPY TO TRACK THE MOVEMENT OF ATOMS ON SURFACES

A thesis submitted in partial fulfilment of the requirements for
the degree of Bachelor of Science

AUTHOR: Jamaal Hassan

STUDENT ID: 201328628

PROJECT SUPERVISORS: Professor Hem Raj Sharma,
PhD Student Dominic Burnie, Professor Ronan McGrath

Declaration

I confirm that I have read and understood the University's Academic Integrity Policy. I confirm that I have acted honestly, ethically and professionally in conduct leading to assessment for the programme of study. I confirm that I have not copied material from another source nor committed plagiarism nor fabricated, falsified or embellished data when completing the attached piece of work.

Signed: Jamaal.H

Date: 15/05/21

Preface

Due to the recent COVID-19 pandemic, all face-to-face teaching at the University of Liverpool was suspended for the majority of the academic year. As a result, it is not possible to physically perform measurements with regards to the scanning tunnelling microscope.

In light of this pandemic, all STM images, LEED patterns, the model phason plane and the model isostructural plane have been provided by PhD student Dominic Burnie. The resulting investigation will therefore place a greater emphasis on the observed quasi-crystalline order rather than go into specifics of apparatus operation.

Acknowledgements

Thank you to Professor Hem Raj Sharma and Professor Ronan McGrath for their supervision and essential advice on the project; considerably grateful to PhD Student Dominic Burnie for providing the data, help and being especially open to any questions I had with regards to analysing the STM data. Finally, thank you to my family for their constant support throughout my time at University.

Abstract

The purpose of this project is to familiarise with the background on imaging techniques, specifically scanning tunnelling microscopy (STM), alongside various image representation software to analyse and understand quasicrystal structure.

The quasicrystal clean surface is first analysed by reproducing the results obtained in a published paper, showing the surface possesses quasi-crystalline order, such as aperiodicity and 5-fold symmetry. This is approached by measuring step heights of terraces with relation to the golden ratio and the Fibonacci sequence. Appropriate comparisons of the STM image to the model plane are made, by using Penrose tiling overlays and comparison with the cluster centres, thus showing the surface possesses quasi-periodic order.

The movement of atoms after metal deposition is analysed and related to appropriate data processes, such as auto correlation and drift correlation. Movement sites of the STM image on the local plane are compared to corresponding sites on the model phason plane, thereby resulting in further verification that movement on the surface is also related to quasi-crystalline nature.

It is found that in the general case, results are successfully verified to published data and the implications of these results related to the quasicrystal structure are discussed.

1. Introduction

1.1 Quasicrystals

Quasicrystals show symmetry (such as five-fold) with aperiodic tiling. They usually have an icosahedral (20-sided) three-dimensional structure. Professor Dan Shechtman discovered the structure in 1982 [1] and it went against what was fundamentally known about crystallography at the time, however he eventually won the Nobel Prize in Chemistry in 2011.

Since its discovery and production, quasicrystals have been a topic of intensive research [2] in surface studies, from producing intricate metal alloys [3] to showing different orders of symmetry [4].

Quasicrystals are characteristically known to have relations to the golden ratio, the Fibonacci sequence, as well as their contrasting nature to conventional crystals. Unlike regular crystals, quasicrystals show aperiodicity and are not translationally symmetric. Their diffraction patterns show higher orders of symmetry and they are known to be hard and brittle. Although individual elements are metallic, they usually exhibit poor conductivity [2].

It is a result of these peculiar qualities that demand further investigation and research. The purpose of this analysis will hopefully further understanding of quasi-crystalline nature and corresponding characteristics. In terms of the i-Ag-In-Yb surface, the project will demonstrate the 5-fold symmetry of the icosahedral structure as well as how aperiodicity and specific patterns apply to quasicrystals.

1.2 Aperiodicity and Symmetry

To understand quasicrystals, it is important to understand the relevant concepts behind their nature. It was previously thought that only two, three, four and six-fold symmetry exist when tiling the plane, as demonstrated by the figure below.

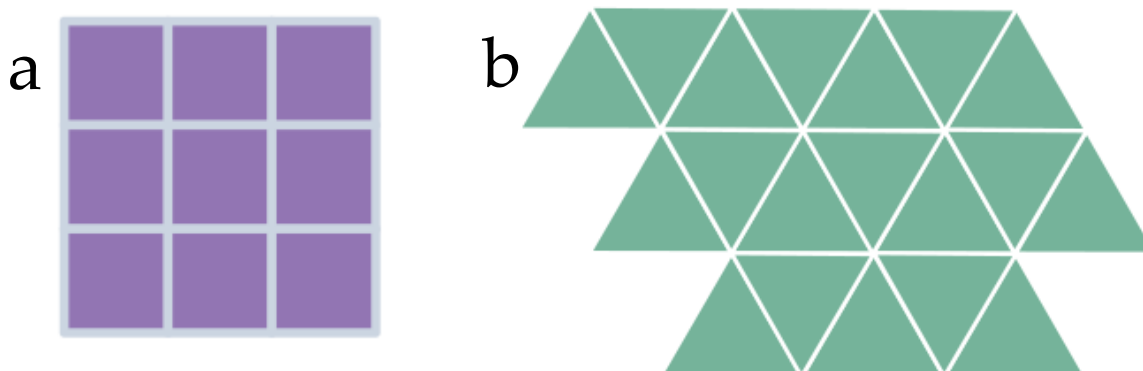


Figure 1.1: a) and b) showing 4-fold and 3-fold symmetry respectively if the pattern were to be extended infinitely across the plane.

The two images highlight patterns of symmetry. Taking Figure a) as an example, if the pattern extended infinitely across the plane, it would be possible to rotate the pattern four times to produce the same pattern, thus giving 4-fold symmetry; a similar case is made for Figure b) possessing 3-fold symmetry.

Both images also possess periodicity, meaning the pattern would repeat itself without any gaps between the constituent shapes across the plane as shown by Figure 1.1. Considering this, aperiodicity would mean that the pattern does not repeat across the plane; taking two subsections of the tiling pattern one would find differences.

No other orders of symmetry were thought possible until in 1974 [5], Sir Roger Penrose proposed an aperiodic 5-fold pattern as shown in the Figure below.

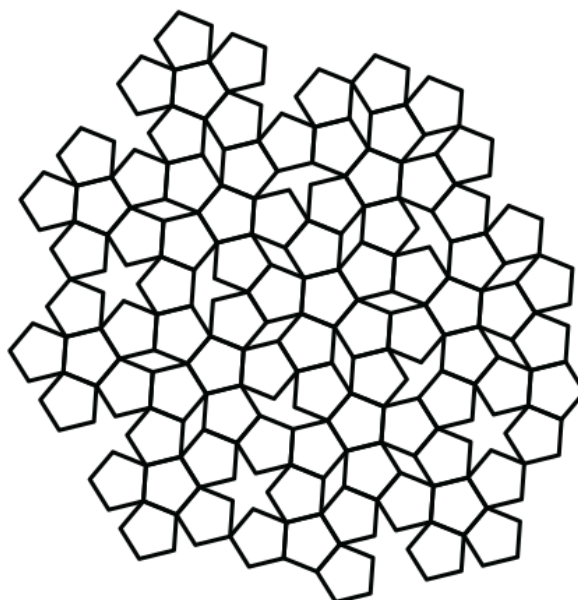


Figure 1.2: Penrose (P1) tiling, showing four shapes that are able to tile the plane aperiodically.

In Figure 1.2, four distinctive shapes are seen: pentagons, five-pointed stars, boats, and diamonds. From these shapes, it is possible to produce an aperiodic pattern with 5-fold symmetry. Penrose eventually was able to reduce this pattern to two shapes, however the main focus of this investigation will be on the P1 tiling.

Regarding quasicrystals, several studies have shown how Penrose tiling is observed in quasicrystals [6] and have also shown how they possess orders of symmetry formerly

thought impossible. However, these features of quasicrystals were further extended into patterns in nature, more specifically the Fibonacci sequence.

1.3 Fibonacci Sequence and the Golden Ratio

The Fibonacci sequence is most well known for being a sequence of numbers, which follow a specific pattern, as shown.

$$0, 1, 1, 2, 3, 5, 8, 13, 21, \dots$$

The sequence above is produced by adding the two consecutive numbers before to produce the next, for example the addition of 3 and 5 produce 8, the addition of 5 and 8 produce 13 and so on. As the sequence progresses it is found that the ratio between two consecutive Fibonacci numbers approach the golden ratio τ ,

$$\tau = \frac{1 + \sqrt{5}}{2} = 1.618033 \dots$$

The golden ratio is an irrational number; its origins date back to the times before Pythagoras [7] and it is a subject of discussion across many areas knowledge. The golden ratio is often associated with patterns in nature, such as taking the ratio of spirals in flowers or how flowers usually have petals corresponding to Fibonacci numbers [8].

Correspondingly, the Fibonacci sequence and golden ratio is readily observed in specific characteristics of quasicrystals as discussed further.

2. Methodology

2.1 Experimental Techniques

2.1.1 Scanning Tunnelling Microscopy

Considering its first use on superconductors [9], scanning tunnelling microscopy (STM) is a fundamental experimental technique used widely in many areas of scientific research, most notably in surface studies [10]; examples include analysing semiconductor surfaces [11] to producing images on the atomic scale [12].

With regards to analysing the surface, scanning tunnelling microscopy is the main imaging technique used. The method relies upon using the principle of quantum tunnelling of electrons between the sample and the tip, as represented by the equation below.

$$J \propto \exp\left(-2\sqrt{\frac{2m\phi}{\hbar^2}}z\right) \quad (1)$$

Where J is the tunnelling current, m is the mass of the electron, ϕ is the effective barrier height, z is the tip-sample separation and \hbar is the reduced Planck's constant [13]. The equation shows that the current is largely affected by the tip-sample distance, which is usually within the range of nanometres (10^{-9} metres) or Angstroms (10^{-10} metres).

In terms of the quantum tunnelling effect, STM relies upon electrons overcoming a potential barrier, by tunnelling from the tip to the sample or vice versa. The direction of tunnelling is dependent on the bias that is applied. For the purpose of this investigation, a negative bias is used meaning the electrons tunnel from the sample to the tip.

The general set-up of the apparatus is represented in the Figure. The diagram highlights how the height of the tip is adjusted using a feedback loop, as well as ensuring the current remains constant when changing the height [14].

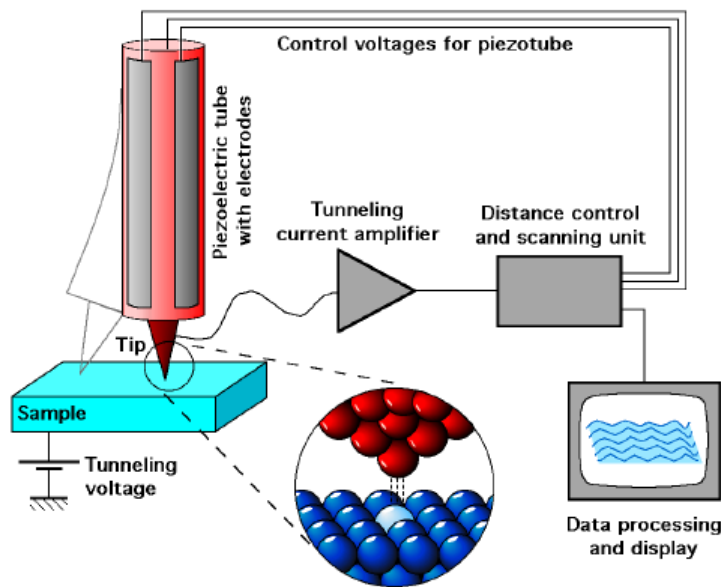


Figure 2.1: Diagram showing general operation of STM apparatus with feedback loop [17]. A piezoelectric drive (electricity produced by pressure or mechanical strain) is used with a tunnelling voltage applied. The tip is usually made from Tungsten.

Considering the overall operation of the apparatus, a constant current mode is usually preferred, and adopted for this particular surface analysis, over a constant height mode. Constant current involves the tip-sample distance to vary in the z -direction, to ensure a constant current is employed when scanning the surface, whereas a constant height mode

means the tip-sample separation remains relatively constant when scanning across the plane. Although a constant height mode has a greater scanning rate than that of constant current, it is often not viable for rough surfaces due to the possibility of physical interaction between the tip and sample. A constant current mode reduces the likelihood of this possibility and ensures safe operation without damaging the surface.

2.1.2 Surface Preparation

Before appropriate measurements, the surface under analysis must first be prepared beforehand according to certain procedures. Specifically, heat treatment or annealing alongside ionised sputtering. Annealing is a process of heat treatment, normally applied to the tip, to remove any impurities from external sources before undergoing STM analysis.

Sputtering is applied to the sample and it involves bombarding ionised particles at the surface to similarly clean the surface. In the case of this investigation, an annealing temperature of 430°C is used applied across a timeframe of 2-3 hours, after which ionised sputtering occurs for 30 minutes on the surface.

2.2 Using the Software

To perform appropriate analysis on the STM images produced, four main forms of software are utilised, as outlined:

- **WSxM** – Data representation and analysis software.
- **Inkscape** – Image corrections and tiling overlays.
- **Igor** – Model visualisation.
- **Gwyddion** – Data visualisation software appropriate for analysing movement sites.

WSxM

This is the main software that is used for the majority of the analysis in this investigation. An example of the software window is shown below; WSxM is capable of performing relevant data processes to STM images, such as Fast Fourier Transforms (FFT), autocorrelations, as well as allowing precise measurements of distances between two points of interest.

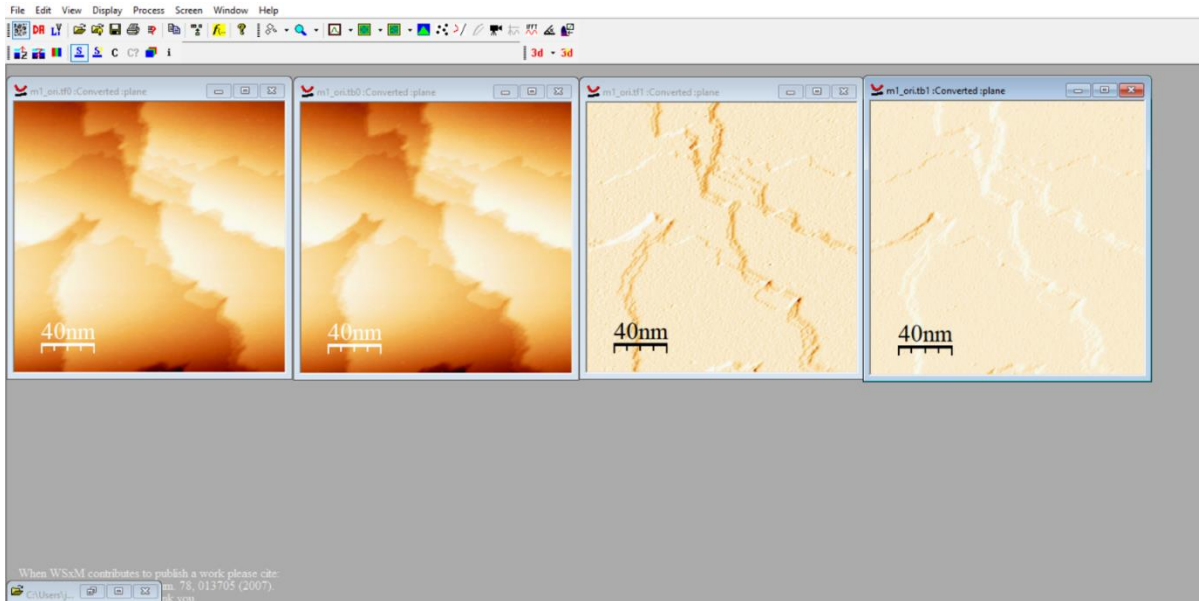


Figure 2.1: Example of WSxM Representation window. From left to right, images represent forward, backward, inverted forward and inverted backward scans.

Inkscape

The software is a vector graphics editor and allows successful Penrose tiling overlays on STM images. Main uses of the software involve performing relevant drift correction to images according to the FFT, as explained further on.

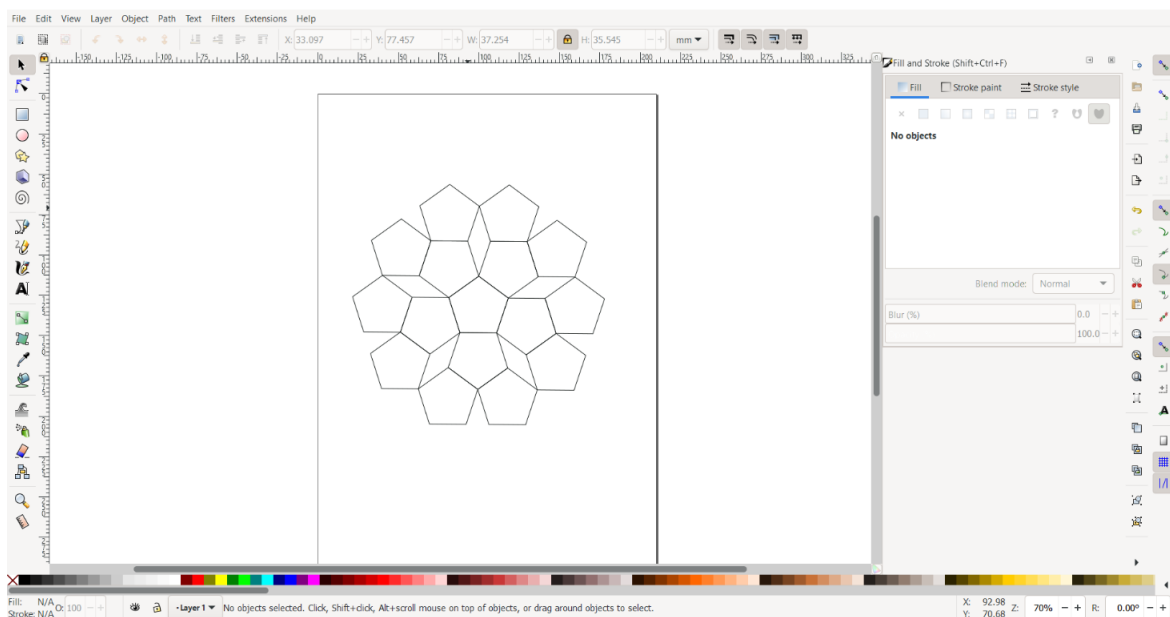


Figure 2.2: Inkscape window. The image is formed from several pentagons, which can be locked together to produce Penrose tiling on prominent features in FFT.

Alongside drift correction and image overlays, Inkscape is utilised largely to determine movement sites between STM images, by allowing overlaps between consecutive frames.

Igor

For comparison, Igor produces a model plane of the sample, highlighting atomic cluster centres and other atomic positions, as well as providing a density of these atoms in the plane.

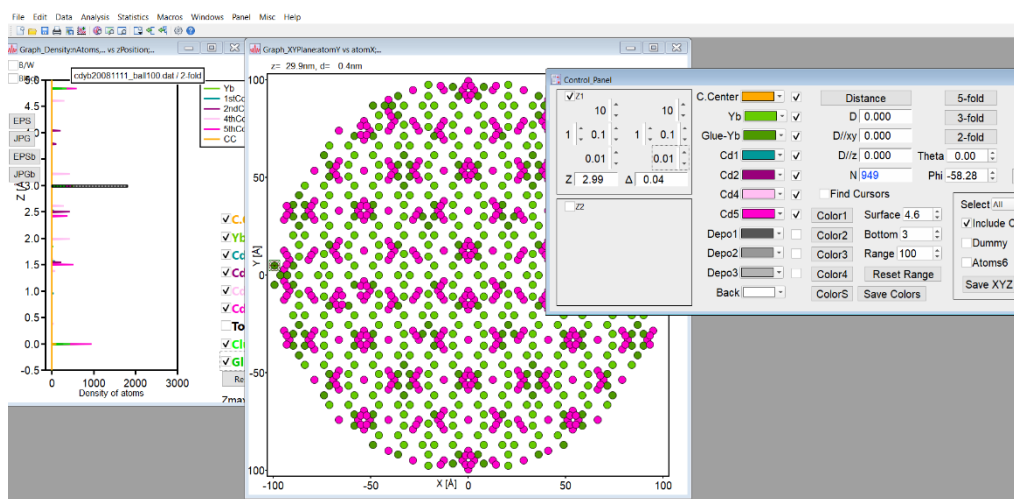


Figure 2.3: Screenshot of Igor window. The figure shows an example of the plane for two-fold symmetry, although it is possible to select higher orders of symmetry, such as five-fold, relevant for this investigation.

Gwyddion

The data visualisation software is most relevant for analysing movement sites. From the images produced in Inkscape, it is possible to perform processes similar to that in WSxM, although the main process utilised is autocorrelation.

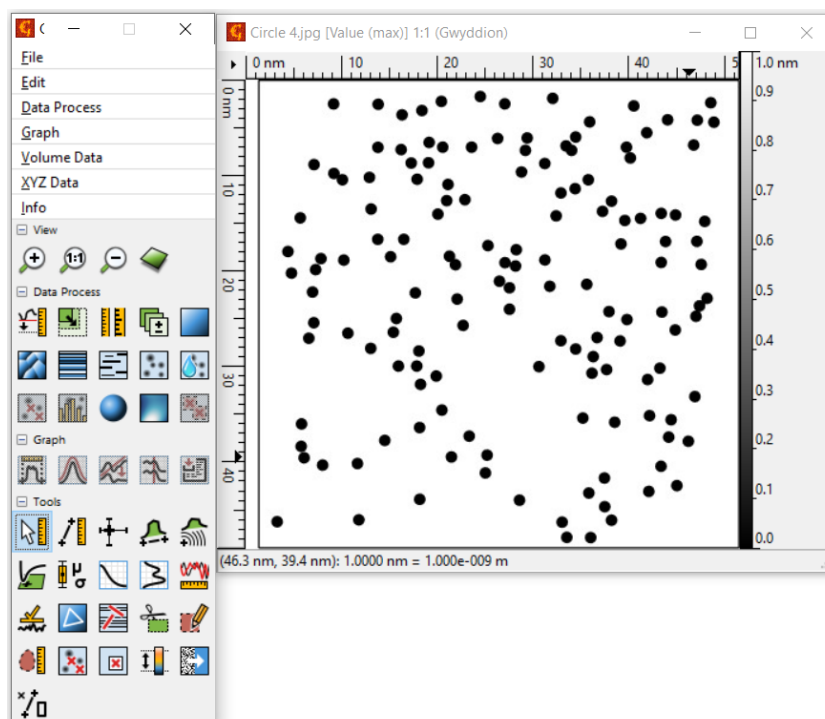


Figure 2.4: Example of the Gwyddion window. The window on the right shows an image from Inkscape from which it is possible to perform an autocorrelation

2.3 Analysing the Clean i-Ag-In-Yb Surface

Before investigating movement on the surface, it is imperative to understand the surface itself before any metal deposition. To ensure this, the results from the analysis are compared to those produced in a published paper [15].

Using a bias dependency of -0.8V and a constant current of 0.175nA , the scans of the clean surface are produced showing the plane split into terraces (Figure 2.5).

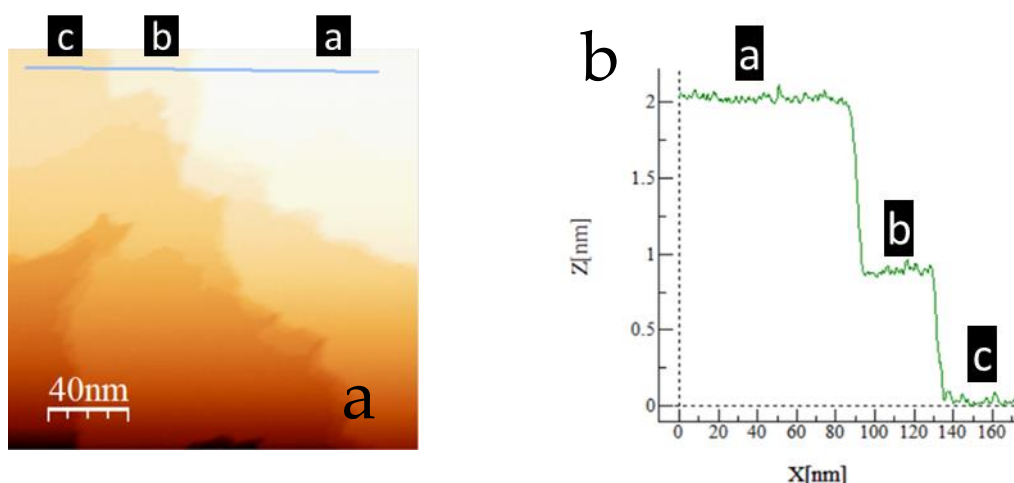


Figure 2.5: a) The image shows a flattened area of the clean surface. The blue line represents a measurement of the step sizes to produce a line profile as shown by Figure b).

The STM image loaded into WSxM is first flattened; this is due to the fact that the tip is slightly inclined to the sample when scanning, meaning the terraces are at different heights than expected. Flattening the image removes the slope of the terraces produced as a result, from which it is viable to make appropriate measurements of the step sizes as shown in the Figure above. However, in a number of the images produced the terraces often congregate into smaller groups, making it difficult to use a line profile due to the smaller surface area from which it is possible to make a measurement.

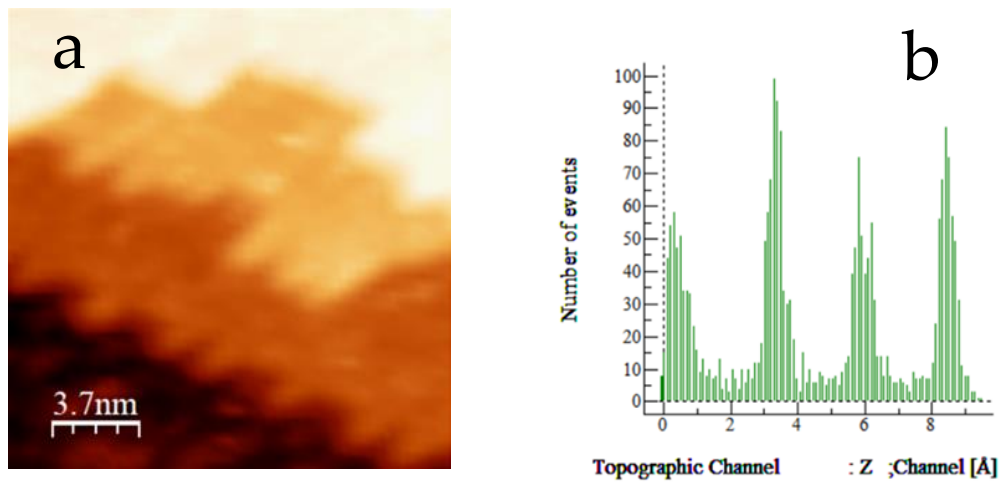


Figure 2.6: a) A magnified region of the clean surface with many terraces. Figure b) A histogram produced showing the distribution of step sizes between the terraces. Measuring between peaks of the histogram produces heights of the

The Figure above shows how a histogram analysis tool is utilised to perform precise measurements of the step sizes. By magnifying regions of interest, specifically with many terraces involved, it is possible to use this data process to increase the overall number of measurements to provide a more reliable analysis.

From these step sizes, a histogram is produced showing the general distribution of heights across the surface (Figure 3.1). Using this data, the occurrences of specific types of terraces are compared to those published [15]. Using these step sizes, quasi-crystalline order is verified by comparing to the model plane in Igor.

2.3.1 FFT and Autocorrelation of the Clean Surface

Apart from the step sizes, quasi-periodicity is demonstrated by performing applicable processes to the STM images themselves.

Fast Fourier Transform (FFT) is an algorithm which computes the frequency domain from the time domain of the image. It splits the image into its real and imaginary parts and is able to compute the image in reciprocal space, as shown in the Figure below.

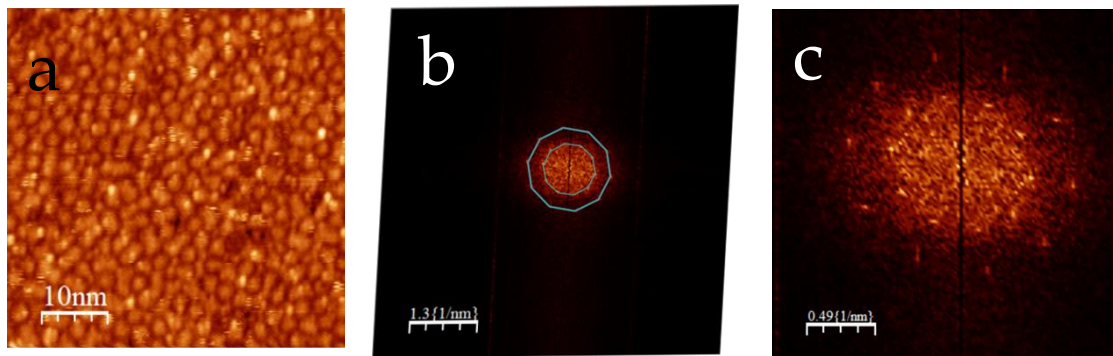


Figure 2.7: a) STM image within the range of angstroms. Figure b) FFT of Figure a) with decagon overlay. Figure c) Magnified central region of FFT. Vertices of decagons should lie at the bright spots.

From the STM image, an FFT is produced allowing a decagon overlay. The decagons are τ -scaled as expected for quasi-crystalline order. Considering the FFT and STM image, important drift corrections are required due to deviations of the tip across the surface. The drift correction is applied by skewing the FFT slightly in order for the vertices of the decagons to lie at the bright spots. From these corrections to the FFT, appropriate adjustments are made to the STM image, taking into account the fact that the FFT is in reciprocal space.

From the FFT, it is possible to only filter the bright spots (Figure 2.7c), allowing the characteristic pentagonal features to be highlighted. Autocorrelation is utilised for the filtered image; the data process is an equation which essentially finds similarities between one image and another. In this investigation, a self-correlation is often used, which finds similar features between the image and the image shifted a small distance on the x, y axes. Measurements of the edge lengths of the protrusions shown in the images are compared to the model to highlight the expected quasi-periodic order.

2.4 Analysing Movement on the i-Ag-In-Yb Surface

Alongside the clean surface, movement on the surface also demonstrates quasi-crystalline order.

Taking into account several STM images taken consecutively across the sample with the same tip conditions, such as bias dependency and current, a movement map is constructed showing major sites of progress across the surface, as shown in the figure below.

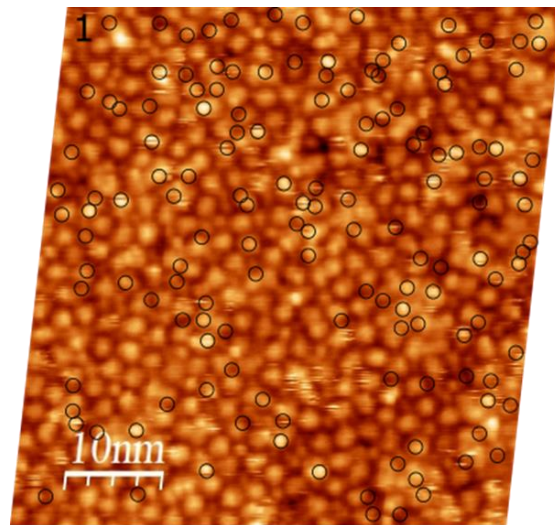


Figure 2.8: STM image with 145 sites of movement recorded across 7 frames, represented by small circles. Tunnelling current is 0.079nA and voltage is -0.8V.

From Figure 2.8, the movement is constructed by overlaying consecutive frames; areas where protrusions seem to disappear or appear between the two frames are highlighted and the process is repeated until all frames are accounted for. Removing the STM image and leaving only the sites of movement (Figure 3.5a), an autocorrelation is performed (through Gwyddion), where the image produced is compared to the autocorrelated STM image.

2.4.1 Comparison to the Phason Plane

With regards to relating the movement of the corresponding images, it is impertinent to mention relations to the phason plane.

Phasons are characteristic of quasicrystals and essentially describe a collection of atoms shifting to new sites. Research into the pattern of this movement is still taking place and could allow feasible predictions into quasicrystal atomic arrangement [16]. In terms of this investigation, movement sites on the local scale are compared to those of the model phason plane by highlighting corresponding locations between the two images.

3. Results and Discussion

3.1 Clean i-Ag-In-Yb Surface

3.1.1 Implications of Step Height Measurements

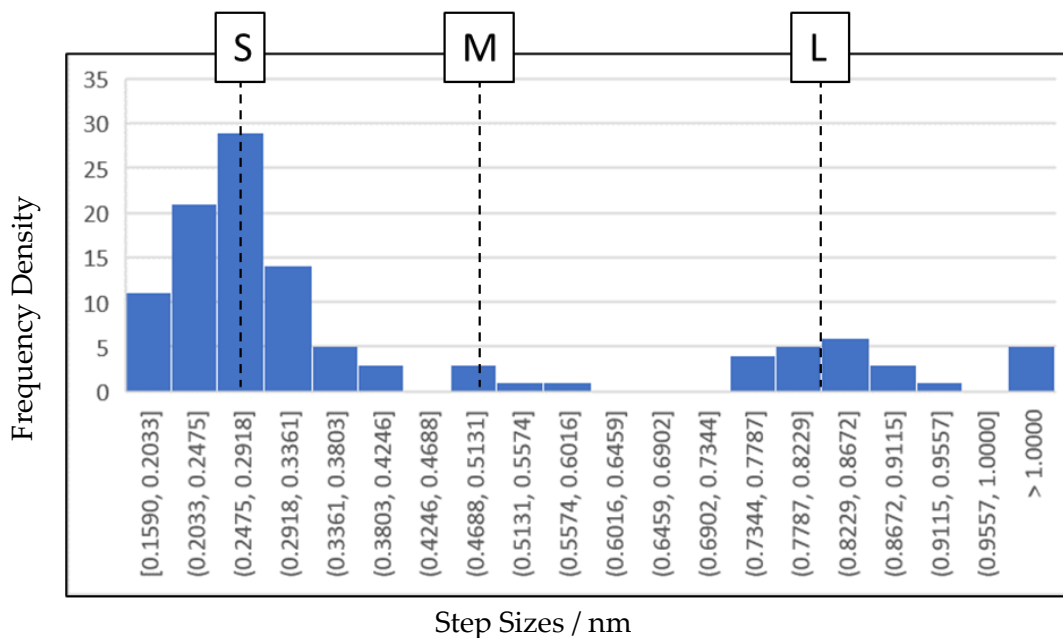


Figure 3.1: Histogram showing distribution of step sizes from 112 measurements. Each area is highlighted to show the type of step sizes available.

From Figure 3.1, the distribution of the heights of the terraces are shown, each labelled with the corresponding step type of short (S), middle (M) and long (L). The measured step height for the S, M and L steps respectively are 0.36 ± 0.01 nm, 0.50 ± 0.02 nm and 0.82 ± 0.03 nm. The expected sizes [15] are 0.28 ± 0.04 nm, 0.58 ± 0.03 nm and 0.85 ± 0.03 nm for the S, M, L steps respectively. Considering the two sets of results, the measured values are consistent (see Appendix A) to the expected.

With regards to the occurrence, the measured values are 73%, 5% and 22% accordingly for the S, M, and L steps, compared to the expected of 66%, 12% and 22%. Step sizes ≥ 1.00 nm are not taken into account as they are usually a combination of the S and L steps.

From these results, although the occurrence between the two sets show discrepancies between the S and M steps, the overall status of these occurrences is observed, with the S steps being the most prevalent and the M steps having the lowest occurrence. In terms of relating these step types to quasi-periodicity, the following equation is obeyed.

$$\frac{\text{Number of L steps}}{\text{Number of S steps}} \approx n\tau \quad (2)$$

Where n is some scalar and τ is the golden ratio. Ratio of the occurrences of the L and S steps between the measured and expected are 0.19 and 0.21 for the scalar value of tau. Although it would be more reasonable to use the number of each corresponding step, the relative agreement between the two ratios of the occurrences show that the experimental results are verified from the published data.

The importance of these step sizes is also seen in the model plane, as shown in the figure below.

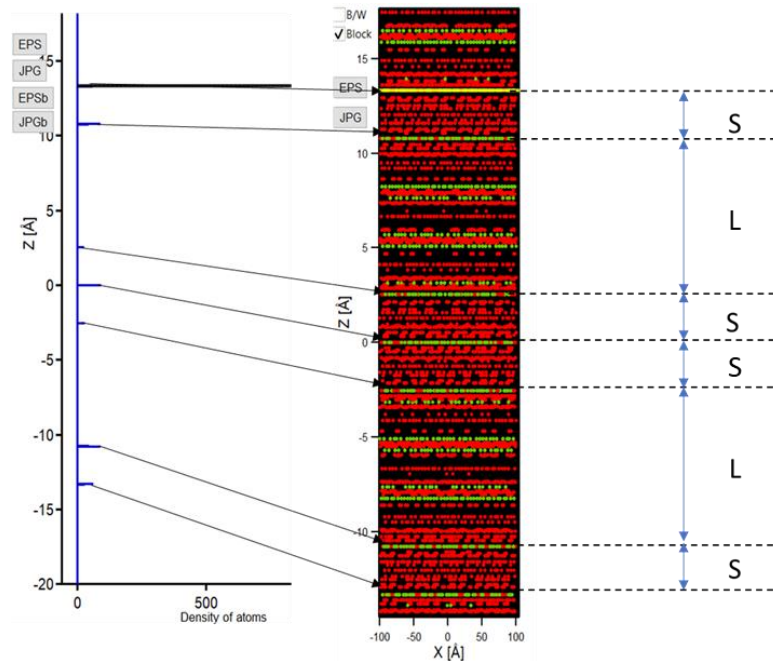


Figure 3.2: Comparison to the model plane, highlighting features of the S and L steps. Red represents the Cd atoms, green represents the Yb atoms and blue is the cluster centre. The figure on the right is a graph of the ZX plane showing the cluster of atoms. The image on the left shows the cluster centres.

Although CD and Yb are used in the model, Ag-In-Yb is considered to be isostructural (similar chemical structure) to this particular model and is sufficient for comparison. From the Figure it is shown that the S and L steps follow the Fibonacci sequence, if the graph were to be expanded. Considering these results of tau-scaling and the Fibonacci sequence, it is reasonable to assume that quasi-crystalline order is observed, with successful verification of these results to the published data.

3.1.2 5-fold Symmetry and Aperiodicity

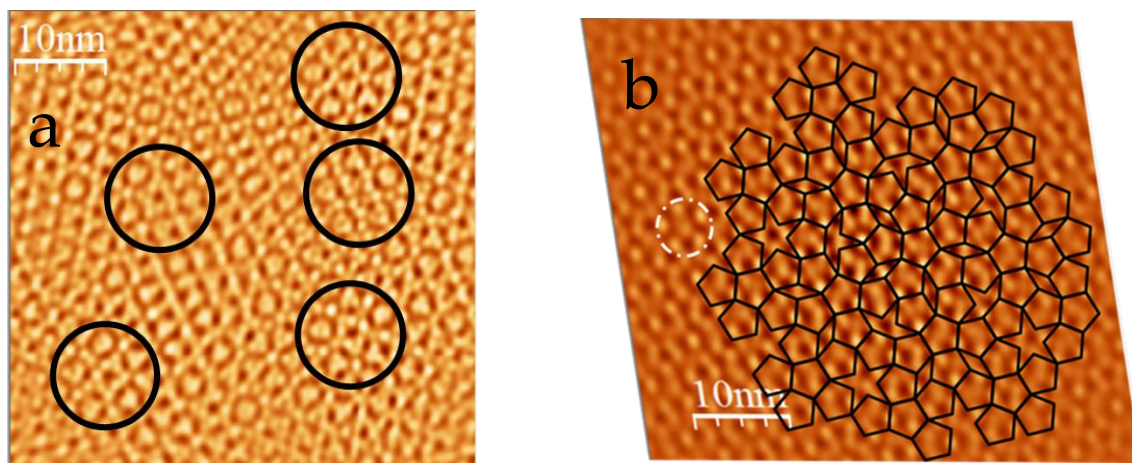


Figure 3.3: a) Filtered image of FFT. Circles highlight pentagonal features. b) P1 tiling overlay after self-correlation of filtered image, white circle shows example of pentagonal feature.

Figure 3.3a) and b) both demonstrate the characteristic 5-fold symmetry of the quasicrystal sample. Figure a) shows clear pentagonal features on the filtered image, whilst figure b) highlights 5-fold symmetrical nature, given by the Penrose tiling overlay. In order to verify with published results [15], the edge lengths of corresponding images are compared.

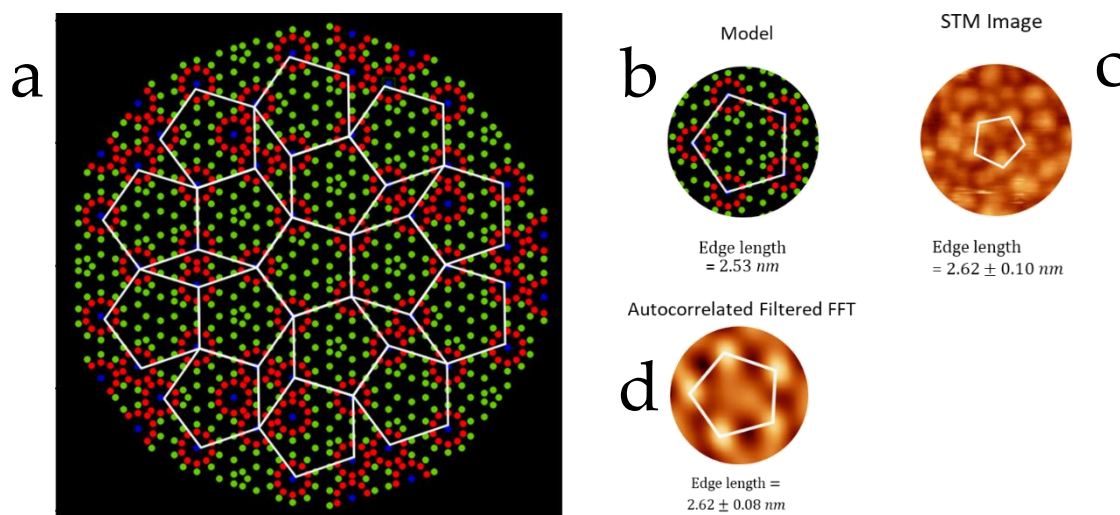


Figure 3.4: a) Model plane with pentagonal overlay. b), c) and d) Edge length measurements and pentagonal overlay of model, STM image and autocorrelated FFT.

Performing a consistency check, all values are in agreement with each other; the expected value from published results [15] is 2.40 ± 0.15 nm. Considering a difference of 9% for the

measured and expected edge length, the results do show agreement considering their respective range in error.

3.2 Movement on i-Ag-In-Yb Surface

3.2.1 Movement Map Autocorrelation Comparison

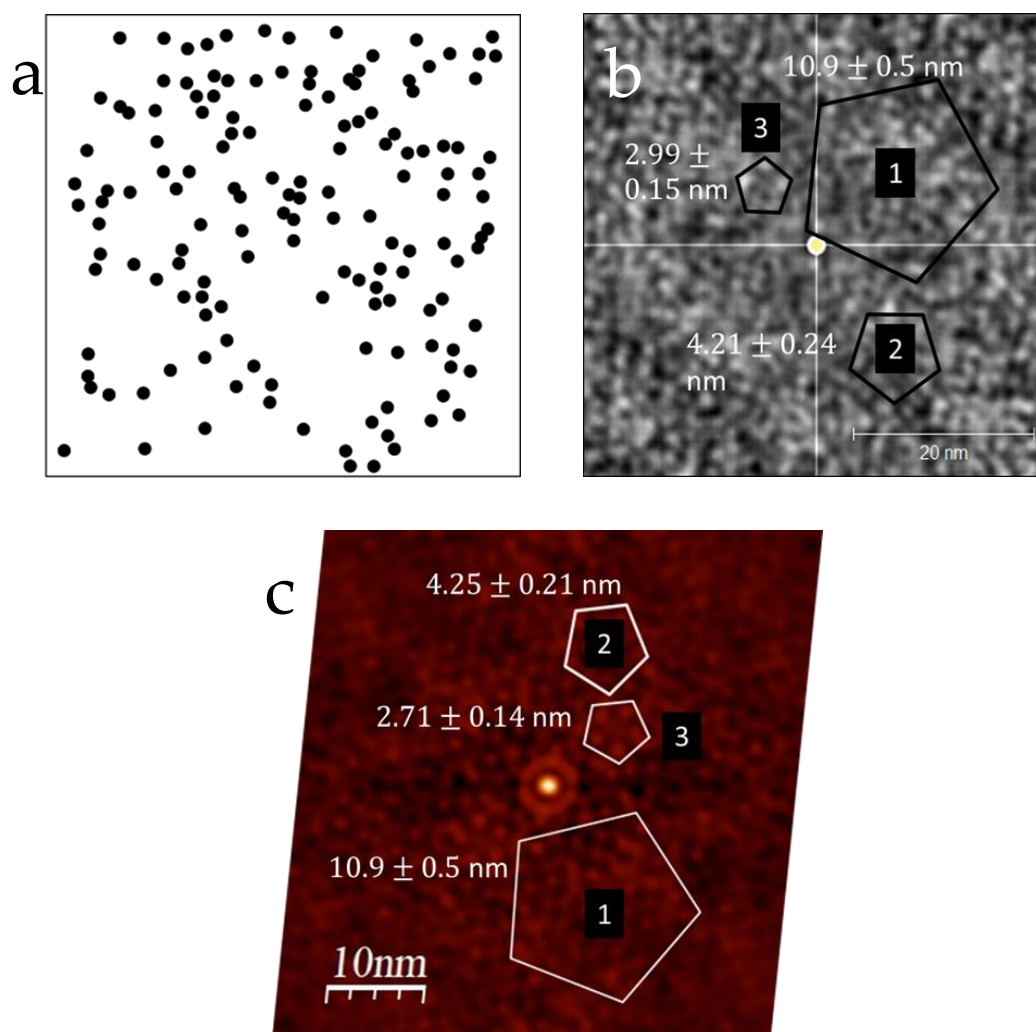


Figure 3.5: a) 51.6 x 51.6 nm area. Movement of 145 sites without STM image. b) Autocorrelation of movement map using Gwyddion. c) Autocorrelation of first frame with applied drift correction.

From Figure 3.5a), an autocorrelation of the movement map is produced (Figure 3.5b). From the image itself, pentagonal features are visible as shown by the protrusions present on the image. Comparisons of the edge lengths to the measured values of Figure 3.5c) show consistency.

In order to demonstrate relevant quasicrystal characteristics, the ratio of side lengths is taken into account to show appropriate tau-scaling. From Figure b) and c) the ratio of the two pentagons labelled 2 and 3 is close to τ , with values of 0.88 and 0.97 scalar multiples respectively. These pentagonal features and tau-scaling show more attributes to quasicrystalline order, as expected of the Ag-In-Yb surface.

3.2.2 The Phason Plane

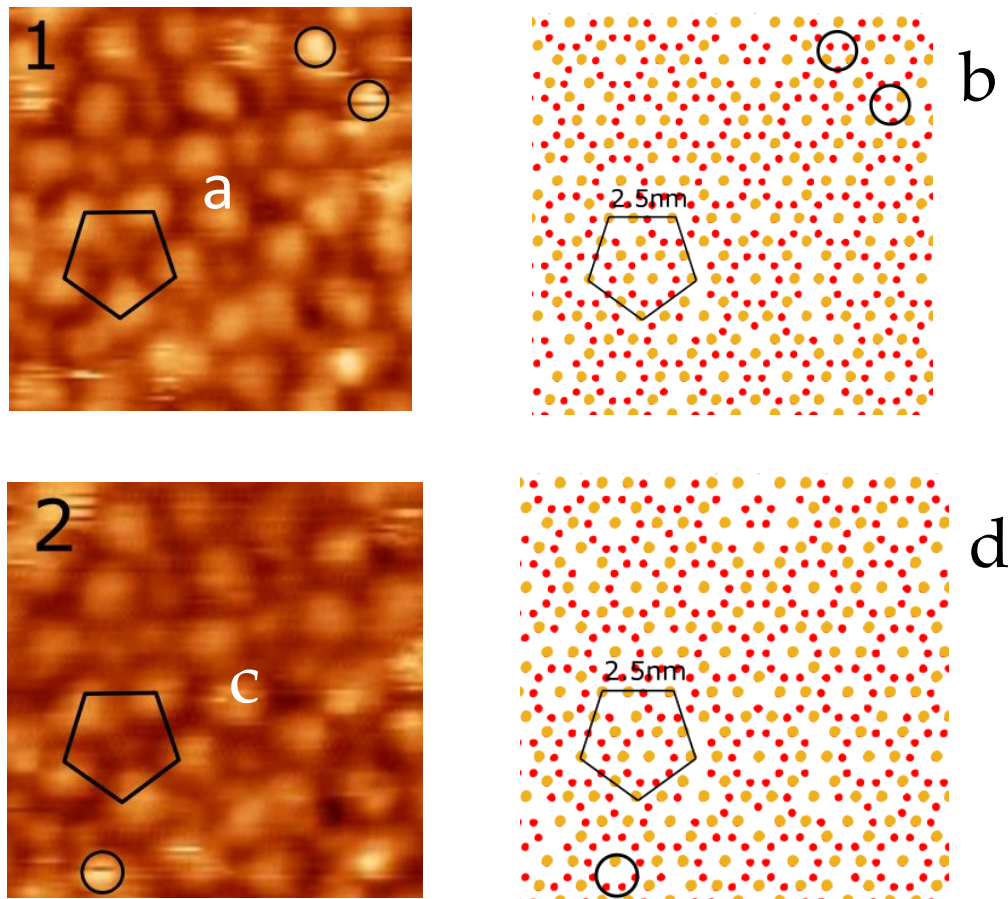


Figure 3.6: a) and c) First and second frames on the local scale of the surface. b) and d) Model phason plane highlighting areas of movement for the first two frames. The yellow circles are cluster centres and the red circles are additional centres connected to phasons.

From the figure above, the collection of movement is observed across the first two frames. This is repeated for each the frames, with each comparison made on the local plane. The areas of movement from one site to the next show the presence of phasons. Although it is difficult to highlight individual cluster centres, the notion of phasons do demonstrate the quasi-periodic nature of movement on the Ag-In-Yb surface as expected.

4. Conclusion

The main outcome of this project was to observe and verify quasi-crystalline order of the i-Ag-In-Yb clean surface and movement on the sample. Over the course of this project, the results have been successfully verified.

However, slight disagreements are present in the specific measurements of the data. Possible reasons for this may be a result of the number of measurements made; increasing this number and taking more observations, if time permitted, would allow a better comparison with published results.

Measuring the distance between two points also presents some challenges. It is often difficult to perfectly align the beginning and end of a measurement (with regards to line profiles and edge lengths) on the centre of protrusions, thus providing inaccuracies between two sets of results. Provided there are no time constraints, it would be possible to obtain an average result from numerous measurements, thus giving a better comparison.

Due to time constraints, it was not entirely possible to completely delve into movement sites with relation to phasons. An appropriate investigation would be to produce a histogram of edge lengths of the movement map, which can then be compared and verified to the expected results.

In terms of the further scope of this project, it is feasible to perhaps look at low-energy electron diffraction (LEED) patterns, which is another way of determining surface characteristics by bombarding the surface with electrons (see Appendix C). Alternatively, other orders of symmetry could be observed, such as 2-fold, and comparisons could be made to higher orders.

With regards to the overall outcome of the project, the investigation has outlined the quasi-crystalline nature of the i-Ag-In-Yb surface, but has also cemented understanding of the structural importance of quasicrystals, as well as their intriguing role in crystallography and surface studies.

Appendix A – Error Propagation

The consistency check used for when comparing two sets of results is outlined below,

$$|x_1 - x_2| < 3\sqrt{\Delta x_1^2 + \Delta x_2^2}$$

Where x_1 and x_2 are the first and second variable; Δx_1 and Δx_2 are their respective errors.

In terms of determining the average step heights from the histograms, the error is taken as the error on the mean, calculated as such,

$$\Delta \bar{x} = \frac{\sigma}{\sqrt{N}}$$

Where $\Delta \bar{x}$, is the error on the mean, σ is the standard deviation and N is the number of measurements.

Appendix B – Additional Tables

Step	Measured / nm	Expected / nm	Measured Occurrence	Expected Occurrence / %
S (Short)	0.26 ± 0.01	0.28 ± 0.04	73	66
M (Middle)	0.50 ± 0.02	0.58 ± 0.03	5	12
L (Long)	0.82 ± 0.03	0.85 ± 0.05	22	22

Table 1b: Table showing complete comparison of distribution heights with expected results.

Ratio	Value	Tau-scaling
1/2	2.56	1.58
1/3	3.64	2.25
2/3	1.42	0.88

Table 2b: Table showing ratio of labelled pentagons of autocorrelated movement map.

Ratio	Value	Tau-scaling
1/2	2.56	1.58
1/3	4.00	2.48
2/3	1.57	0.97

Table 3b: Table showing ratio of labelled pentagons of autocorrelated STM image.

Appendix C - Comments and Questions

Reviewer 1, Question 1: Describe and explain, with an example, similarities and differences expected between Fourier transforms of STM images and low energy electron diffraction patterns.

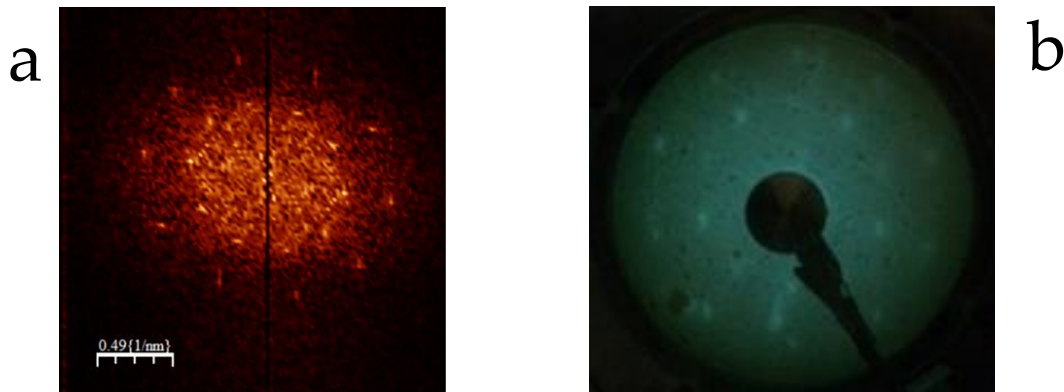


Figure 1c: a) FFT of STM image. b) Low-energy electron diffraction (LEED) of STM image.

Response, Question 1: The figure above shows an FFT on the left and a magnified LEED pattern on the right. From observation, both images show spots corresponding to decagon vertices and are τ -scaled, although the spots on the LEED pattern are slightly faint. The main differences between the two is that the FFT is in reciprocal space, so if a measurement were to be made between two bright spots the inverse of this distance would be considered to be the actual value in real space. For LEED, the image represents a diffraction pattern so it would be possible to make observations without converting from reciprocal space and comment directly on the symmetry of the surface.

Reviewer 1, Question 2: Explain, preferably with a diagram, the physical origin of the "middle"-sized steps. From the presentation, it seems that only short and long steps are expected - is that correct or not?

Response, Question 2: I am not entirely sure on the physical origin of the M step; one possible idea is that the M steps are formed from a collection of S steps and it is not possible to measure precisely the steps sizes, due to the small area of these terraces. M steps are expected when scanning the surface, but usually S and L steps are often taken into greater consideration as they have a greater occurrence across the surface. Although this investigation is limited to analysing the S and L steps, the presence of M steps do warrant significant investigation and would be something that would require analysis and further knowledge if carried on in a later study.

Reviewer 1, Comment 1: Slides are a little text heavy. Delivery is slightly too fast at the beginning, but is then well paced. Excellent animations to explain concepts. Good timing.

Response, Comment 1: The slides are text heavy and I would have preferred to have spread the information across more slides. However, there was concern in overrunning past the 10-minute mark, so it is unfortunate that the information was presented in such a condensed format. However, it is helpful to know the animations proved useful and knowing for next time it would perhaps be easier to try and spread the information out or be more concise when talking about a particular section.

Reviewer 2, Comment 1: Some images or other things to break up pages of text at start. Good use of images later. In a short talk do not need spend time on the outline slide. Clear discussion of the methods and results so far. Too much introductory material, compensated by speaking too fast and skipping through slides too fast to read. Did explain the material well, although the results were skipped through much too fast, so the results were unconvincing as a result.

Response, Comment 2: There was lot more information than previously thought to cover in the presentation. Within the presentation, there was a balance of trying to maintain understanding of the basic concepts whilst undertaking any discussion into the results. I have noticed that more emphasis is placed on the introductory material listening back to the presentation, but it was more as a result of worrying to ensure the concepts behind the project are fully understood. It would have been preferable to have elaborated more on the results and this may have been achieved by reducing time spent on introductory material.

Bibliography

- [1] Shechtman D, Blech I, Gratias D, Cahn JW. Metallic phase with long-range orientational order and no translational symmetry. *Physical review letters*. 1984 Nov 12;53(20):1951.
- [2] Janot C. Quasicrystals. In *Neutron and Synchrotron Radiation for Condensed Matter Studies 1994* (pp. 197-211). Springer, Berlin, Heidelberg.
- [3] Dubois JM. Properties-and applications of quasicrystals and complex metallic alloys. *Chemical Society Reviews*. 2012;41(20):6760-77.
- [4] Levine D, Steinhardt PJ. Quasicrystals: a new class of ordered structures. *Physical review letters*. 1984 Dec 24;53(26):2477.
- [5] Penrose R. Pentaplexity a class of non-periodic tilings of the plane. *The mathematical intelligencer*. 1979 Mar 1;2(1):32-7.
- [6] Bursill LA, Lin PJ. Penrose tiling observed in a quasi-crystal. *Nature*. 1985 Jul;316(6023):50-1.
- [7] Dunlap RA. *The golden ratio and Fibonacci numbers*. World Scientific; 1997.
- [8] National Geographic. *The Golden Ratio*.
<https://www.nationalgeographic.org/media/golden-ratio/> (Accessed 15/05/21)
- [9] Giaever I. Energy gap in superconductors measured by electron tunneling. *Physical Review Letters*. 1960 Aug 15;5(4):147.
- [10] Binnig G, Rohrer H. Scanning tunneling microscopy. *Surface science*. 1983 Mar 2;126(1-3):236-44.
- [11] Kubby JA, Boland JJ. Scanning tunneling microscopy of semiconductor surfaces. *Surface science reports*. 1996 Dec 1;26(3-6):61-204.
- [12] Hansma PK, Elings VB, Marti O, Bracker CE. Scanning tunneling microscopy and atomic force microscopy: application to biology and technology. *Science*. 1988 Oct 14;242(4876):209-16.
- [13] Tunnelling Equation: Kittel C, *Introduction to Solid State Physics*, 8th Edition, 2005
- [14] H.R Sharma. Lecture Notes
- [15] Sharma HR, Shimoda M, Sagisaka K, Takakura H, Smerdon JA, Nugent PJ, McGrath R, Fujita D, Ohhashi S, Tsai AP. Structure of the fivefold surface of the Ag-In-Yb icosahedral quasicrystal. *Physical Review B*. 2009 Sep 3;80(12):121401
- [16] Ziga Lisa. Phys.org. *What do phasons look like?* 2012. <https://phys.org/news/2012-06-phasons.html> (Accessed 15/05/21)
- [17] Scanning Tunnelling Microscopy.
[https://chem.libretexts.org/Bookshelves/Analytical_Chemistry/Book%3A_Physical_Methods_in_Chemistry_and_Nano_Science_\(Barron\)/08%3A_Structure_at_the_Nano_Scale/8.03%3A_Scanning_Tunneling_Microscopy](https://chem.libretexts.org/Bookshelves/Analytical_Chemistry/Book%3A_Physical_Methods_in_Chemistry_and_Nano_Science_(Barron)/08%3A_Structure_at_the_Nano_Scale/8.03%3A_Scanning_Tunneling_Microscopy) (Accessed 15/05/21)